1970 (unpublished).
[9]J. D. Harvey and R. C. Johnson, to be published.
[10]F. D. Santos, Ph. D. thesis, University of London, 1968 (unpublished). A report by J. D. Harvey and F. D. Santos giving a full account of the code, which incorporates deuteron *D*-state effects, can be obtained by writing to RCJ.
[11]P. J. A. Buttle and L. J. B. Goldfarb, Proc. Phys. Soc. (London) A83, 701 (1964); G. Bencze and J. Zimanyi, Phys. Letters 9, 246 (1964); F. G. Perey and D. Saxon, *ibid.* 10, 107 (1964).
[12]F. D. Bechetti, Jr., and G. W. Greenlees, Phys. Rev. 182, 1190 (1969).
[13]N. S. Chant and J. M. Nelson, Nucl. Phys. A117, 385 (1968).
[14]N. S. Chant, P. S. Fisher, and D. K. Scott, Nucl. Phys. A99, 669 (1967).
[15]R. C. Kozub, L. A. Kull, and E. Kashy, Nucl. Phys. A99, 540 (1967).
[16]J. L. Snelgrove and E. Kashy, Phys. Rev. 187, 1246, 1259 (1969).
[17]G. R. Satchler, private communication, 1969.
[18]G. R. Satchler, Nucl. Phys. 85, 273 (1966).
[19]N. Austern, Ann. Phys. (N.Y.) 15, 99 (1961).
[20]R. M. Drisko, G. R. Satchler, and R. H. Bassel, Phys. Letters 5, 348 (1963).
[21]B. M. Preedom, J. L. Snelgrove, and E. Kashy, Phys. Rev. C 1, 1132 (1970).
[22]G. H. Rawitscher, Phys. Rev. 163, 1223 (1967); 181, 1518 (1969).
[23]M. Ichimura, M. Kawai, T. Ohmura, and B. Imanishi, Phys. Letters 30B, 143 (1969), and references therein.

PHYSICAL REVIEW C VOLUME 3, NUMBER 2 FEBRUARY 1971

Nuclear Level Densities and Reaction Mechanisms from Continuum Neutron Spectra*

S. M. Grimes, J. D. Anderson, J. W. McClure, B. A. Pohl, and C. Wong
Lawrence Radiation Laboratory, University of California, Livermore, California 94550
(Received 14 September 1970)

The neutron spectra produced by the $^{51}V(p,n)^{51}Cr$, $^{59}Co(p,n)^{59}Ni$, $^{48}Ti(\alpha,n)^{51}Cr$, and $^{56}Fe(\alpha,n)^{59}Ni$ reactions were measured at five angles between 15 and 135° for proton energies between 7.8 and 14.7 MeV, and for α energies between 11.5 and 22.7 MeV. Spectra at low energies were used to obtain the spin-weighted level density of the residual nuclei ^{51}Cr and ^{59}Ni. Comparison of these spectral shapes with those obtained at higher energies made possible a separation of the higher-energy spectra into compound and noncompound contributions.

The deduced compound-nuclear cross sections to given groups of levels were related to the integrals of the level densities of the residual nuclei; the variation of these cross sections with energy was used to extend the level-density measurements beyond the neutron binding energy. A constant-temperature level-density form is found to be appropriate for ^{51}Cr and ^{59}Ni up to residual excitation energies of 14 MeV. Values of the moment of inertia of the residual nuclei were extracted from the magnitude of the asymmetry of the compound-nuclear angular distributions. The characteristics of the noncompound portion were compared with those expected from direct- and pre-equilibrium-reaction mechanisms. It is concluded that no convincing evidence for a pre-equilibrium component is observed in the (α,n) spectra; the (p,n) data show behavior consistent with contributions from both pre-equilibrium- and direct-reaction mechanisms. A value of approximately 160 keV was obtained for the widths of the participating doorway states from a model-dependent calculation based on the magnitude of the pre-equilibrium (p,n) cross section.

I. INTRODUCTION

Analyses of nuclear emission spectra have yielded much information about nuclear level densities, including both the functional form and parameters of the level-density distribution for specific nuclei.[1-7] The statistical theory[8] predicts that the differential cross section for emission of particles of energy E integrated over angle can be related to the level density $\rho(U)$ of the residual nucleus as follows:

$$\sigma(\epsilon) \propto \epsilon\sigma_c(\epsilon)\rho(U), \quad (1)$$

where ϵ is the channel kinetic energy and $\sigma_c(\epsilon)$ is the capture cross section for the inverse reaction at an energy ϵ.

The consequence of the statistical theory is that nuclear level-density parameters obtained for a specific residual nucleus should be independent of (1) bombarding energy, and (2) entrance channel. Experimental results,[1,2,5,7] however, have sometimes contradicted this prediction. Often, individual spectra have been fit with a specific level-density form, but the parameters so obtained have depended on bombarding energy as well as residual excitation.

In addition to the excess of high-energy particles produced by direct reactions, i.e., above the num-

ber expected from statistical theory, it has been suggested[2] that some of the particles observed are produced by pre-equilibrium decay of the compound nucleus. A specific model for such pre-equilibrium emission has been proposed by Griffin.[9] The compound nucleus is considered to be formed as the result of a number of two-body interactions, each of which leads to a more complicated configuration. If each of these states is assumed to have a small width for particle emission in addition to its width for decay into a more complicated configuration, a pre-equilibrium component will be generated. Griffin calculates the shape of such a spectrum and shows that the Sn-(p,n) data of Wood, Borchers, and Barschall[5] can be fit with an expression including a pre-equilibrium component and an evaporation term. Modifications of the theory have been proposed by Blann[10] and Williams,[11] and Blann, Lanzafame, and Bowman[12] have shown that the model can fit the excitation functions for some α-induced reactions between 20 and 100 MeV.

The present measurements were undertaken in an effort to determine if the emission spectra produced in various reactions leading to the residual nuclei ^{51}Cr and ^{59}Ni show evidence of nonequilibrium contributions and, if observed, to compare these portions of the spectra to the predictions of the intermediate structure model. The technique of analysis used also provided estimates of the direct-reaction contributions to the neutron yield. Stripping off these two noncompound components from the measured spectra yielded the compound-nucleus component of the spectrum; the bombarding energy dependence of this portion of the spectrum was used to extend the deduced level-density measurements up to 16-MeV residual excitation.

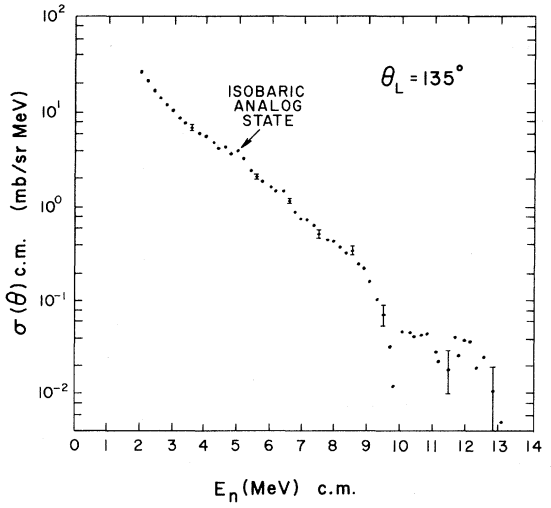

FIG. 1. The differential cross section for the ^{59}Co(p,n)-^{59}Ni reaction as a function of center-of-mass neutron energy. The bombarding energy was 14.7 MeV and the laboratory angle was 135°. Indicated errors are statistical only.

II. EXPERIMENTAL PROCEDURE

The reactions studied included ^{48}Ti$(\alpha,n)^{51}$Cr, ^{51}V$(p,n)^{51}$Cr, ^{56}Fe$(\alpha,n)^{59}$Ni, and ^{59}Co$(p,n)^{59}$Ni. The experimental arrangement and electronics have been described previously.[13] Protons with energies between 7.8 and 14.7 MeV and α particles between 11.5 and 22.7 MeV were produced by the Livermore 90-in. variable-energy cyclotron. The

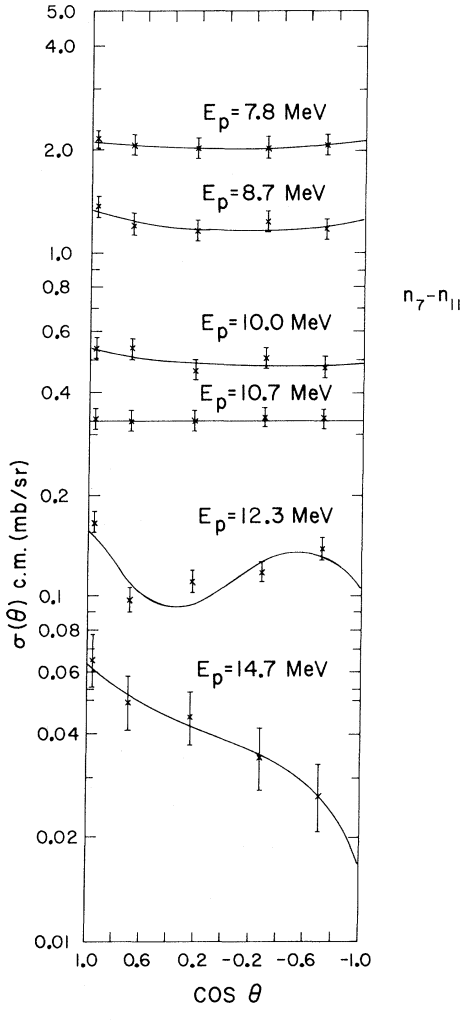

FIG. 2. Angular distribution of the neutrons produced in the ^{59}Co$(p,n)^{59}$Ni reaction leaving ^{59}Ni in five excited states ($1.69 \leq U \leq 1.96$ MeV) as a function of bombarding energy. Indicated errors are statistical only. The observed change from an isotropic to a forward-peaked angular distribution is consistent with the expected transition from a compound-nuclear to a direct-reaction mechanism.

charged particles impinged on solid self-supporting targets and the resulting neutrons were detected in NE 213 scintillators. Neutron energies were determined from the time of flight over a 10.8-m flight path. γ-produced background was reduced by exploiting the pulse-shape discrimination properties of NE 213, and pulses produced by recoil protons with energies less than 1.6 MeV were eliminated with a linear bias. The use of five detectors enabled the simultaneous accumulation of data for angles at 30° intervals between 15 and 135°. A typical (p,n) spectrum is shown in Fig. 1.

III. DATA REDUCTION AND ANALYSIS

A. Compound-Nuclear Processes and Level Densities

The differential energy spectra for the highest-energy neutrons showed peaks at nearly all bombarding energies; these corresponded to low-lying levels or groups of levels in the residual nuclei. Examination of the angular distributions of these neutrons indicated that the predominant reaction mechanism changed from compound nuclear at the lowest to direct reaction at the highest bombarding energies. Figures 2 and 3 show the transition in the angular-distribution shape as a function of bombarding energy for one such peak in both the (p,n) and (α,n) spectra. The isotropic angular distribution at low energies is presumed to be due to a compound-nuclear reaction mechanism. Either a compound-nuclear or a mixture of pre-equilibrium and compound mechanisms would be consistent with the symmetric distribution observed at higher energies (see Appendix A), while the forward peaking at the highest energies is probably due to direct processes. Essentially the same transitions can be observed as a function of outgoing neutron energy at a specific bombarding energy, as can be seen in Fig. 4.

With the exception of the isobaric analog state in the (p,n) spectra, no peaks corresponding to specific levels were observed for neutrons corresponding to residual excitations greater than 3

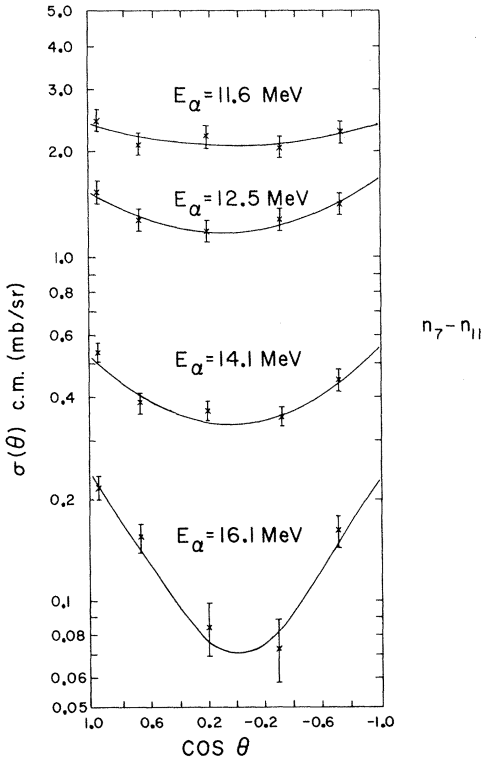

FIG. 3. Angular distribution of the neutrons produced in the ^{56}Fe$(\alpha,n)^{59}$Ni reaction leaving ^{59}Ni in five excited states ($1.69 \leq U \leq 1.96$ MeV) as a function of bombarding energy. This is the same neutron "group" shown in Fig. 2 for the (p,n) reaction. Indicated errors are statistical only. The symmetry observed at each of these bombarding energies indicates that direct processes are not contributing appreciably to the cross section to these levels in this energy region.

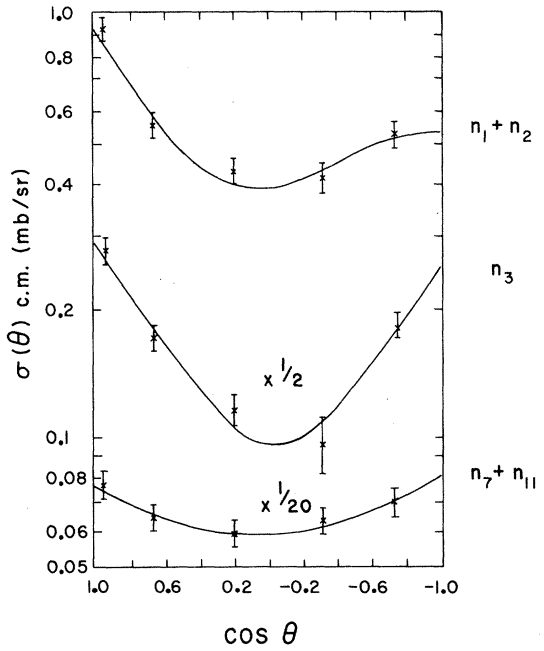

FIG. 4. Angular distributions for three neutron "groups" produced in the ^{56}Fe$(\alpha,n)^{59}$Ni reaction at a bombarding energy of 12.5 MeV. The group labeled n_1+n_2 populated two levels in ^{59}Ni ($U=0.34$ and $U=0.47$ MeV), while the n_3 group corresponds to one level ($U=0.87$ MeV) and the n_7-n_{11} group corresponds to 5 levels ($1.69 \leq U \leq 1.96$ MeV). Indicated errors are statistical only. The differences in angular distribution are consistent with the expected transition from a compound-nuclear to a direct-reaction mechanism as the out-going neutron energy increases.

MeV. This portion of the spectra was analyzed by calculating the "channel" cross section

$$\sigma(\theta, \epsilon) = [(A+1)/A]\sigma(\theta, E_n)_{\text{c.m.}}, \quad (2)$$

where A is the mass number of the residual nucleus, $\epsilon = \{[(A+1)/A]E_n\}_{\text{c.m.}}$ is the channel kinetic energy, and $\sigma(\theta, E_n)_{\text{c.m.}}$ is the center-of-mass cross section for the reaction. If the capture cross section $\sigma_c(\epsilon)$ is assumed to be constant, then $[(1/\epsilon)\sigma(\theta, \epsilon)]$ will be proportional to the level density of the residual nucleus according to Eq. (1). Specifically, the assumption of a constant-temperature form for the level density leads to the prediction that a plot of $\log[(1/\epsilon)\sigma(\theta, \epsilon)]$ against U should yield a straight line with slope $1/T$. For a typical Fermi-gas form, a straight line would be obtained from a plot of $\log[(U^2/\epsilon)\sigma(\theta, \epsilon)]$ against $U^{1/2}$.

Because the detector efficiency changed rapidly with energy for energies near the bias, neutrons with energies less than 2.5 MeV were not included in the analysis. Also, no level-density fit was attempted for values of U less than 3 MeV, since discrete levels or groups of levels were observed in the spectra in this region. Spectra for both a forward angle (15°) and a backward angle (135°) are shown for a number of proton and α bombarding energies in Figs. 5–8. The spectra for proton bombarding energies of 10 MeV and below were essentially isotropic in the continuum region ($U \geq 3$). Symmetry about 90° rather than isotropy was observed for proton energies of 10.7 and 12.3 MeV, and a slight forward peaking was present in the spectra corresponding to proton energies of 13.2 and 14.7 MeV.

The (α, n) reaction produced an isotropic angular distribution in the continuum only for α energies of 12 MeV or less. Between 12 and 16 MeV the angular distributions were symmetric rather than isotropic. Ericson and Strutinski[14] have shown

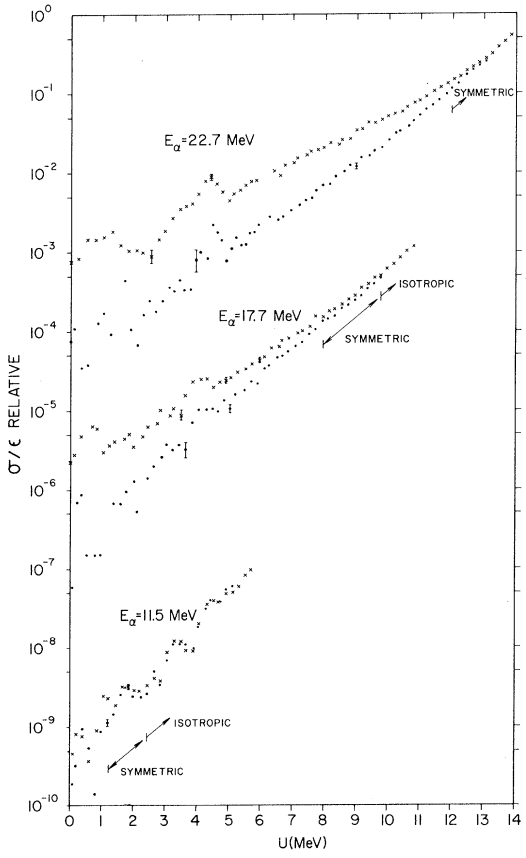

FIG. 5. Neutron spectra from the $^{48}\text{Ti}(\alpha, n)^{51}\text{Cr}$ reaction at three bombarding energies. The points labeled × are at 15°; those labeled • are at 135°. Indicated on each spectrum are the regions in which the angular distribution was symmetric or isotropic.

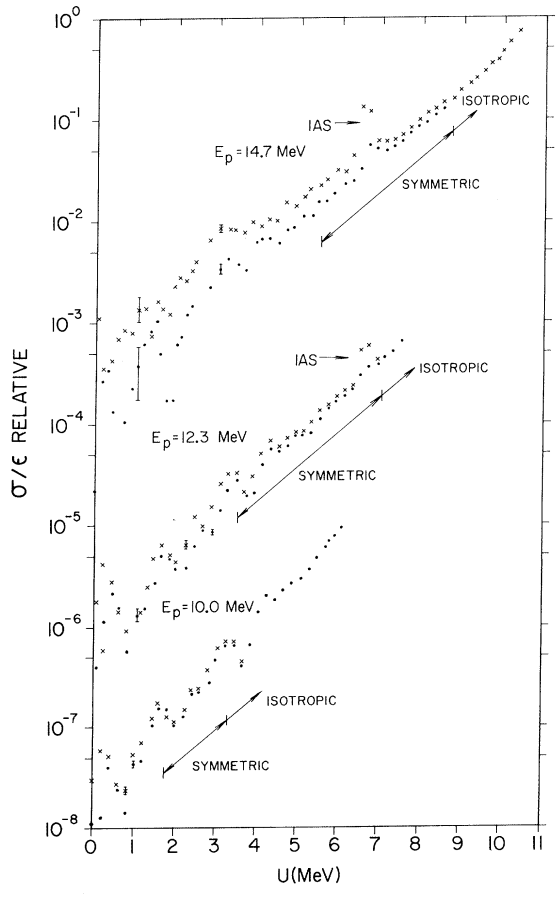

FIG. 6. Neutron spectra from the $^{51}\text{V}(p, n)^{51}\text{Cr}$ reaction at three bombarding energies. The points labeled × are at 15°; those labeled • are at 135°. Indicated on each spectrum are the regions in which the angular distribution was symmetric or isotropic. The isobaric analog state produced the peak marked IAS.

that in general the angular distribution produced by a compound-nuclear reaction in the region of overlapping levels will not be isotropic but will have the form

$$\sigma(\theta) = A(1 + \eta \cos^2\theta), \tag{3}$$

where

$$\eta = I_b^2 I_n^2 / 2(2\sigma^2)^2\hbar^4 = \mu_b E_b \mu_n E_n / 2(2\sigma^2)^2\hbar^4.$$

I_b and I_n are the average angular momenta brought into and removed from the compound nucleus, respectively, R is the radius of the residual nucleus, μ_b and μ_n are the masses of the incoming and outgoing particles, respectively, and E_b and E_n are the corresponding energies, and σ is the spin cutoff parameter in the level-density distribution for the residual nucleus. If η were constant for a given bombarding energy, the correct temperature could be calculated at any angle. Since η is a linear function of outgoing kinetic energy, it can be shown that

$$1/T = 1/T_{\text{app}} - K(\tfrac{1}{3} - \cos^2\theta), \tag{4}$$

where T_{app} is the apparent temperature obtained from a spectrum at an angle θ, and K is the constant in the equation $\eta = KE_n$. The corrected temperature yielded by this relation is the value which would be obtained from analysis of the neutron spectrum integrated over angle. The η values obtained from the (α, n) spectra were approximately linear functions of the neutron energy, while those for the (p, n) reaction were sufficiently small so that no correction was necessary. The (α, n) temperatures shown in Table I have been corrected in accordance with Eq. (4); these corrections were always less than 8%.

Examination of Table I and Figs. 9 and 10 shows that the (α, n) and (p, n) spectra show behavior consistent with the predictions of the compound-nuclear model only for the lower bombarding energies. Figures 9 and 10 are plots of the 135° spectra for proton energies between 7.8 and 12.3 MeV and α energies between 11.5 and 16 MeV. In each figure the line drawn through the spectra is the one obtained by connecting the data points for the appropriate 12.3-MeV (p, n) spectrum. Indicated on the 12.3-MeV (p, n) spectra are the straight lines corresponding to the average temperature

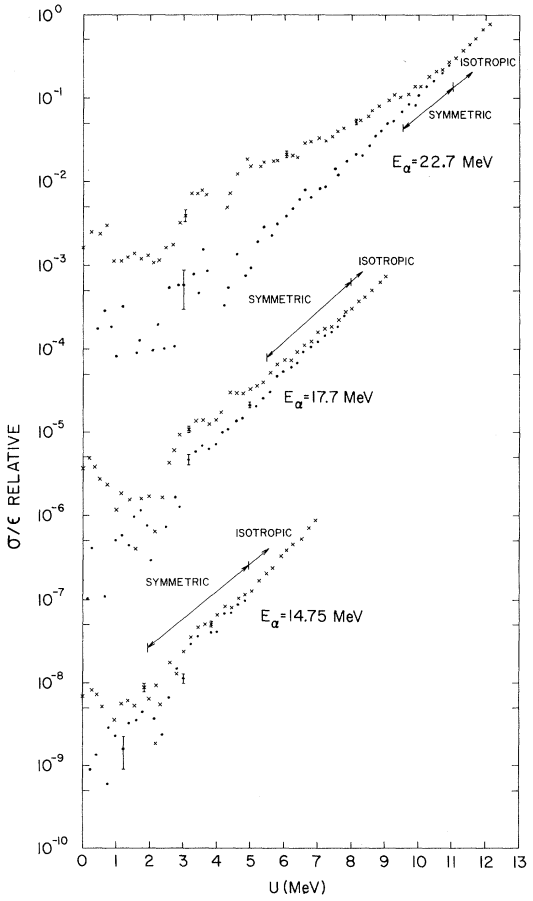

FIG. 7. Same as Fig. 5 for ^{56}Fe$(\alpha, n)^{59}$Ni reaction.

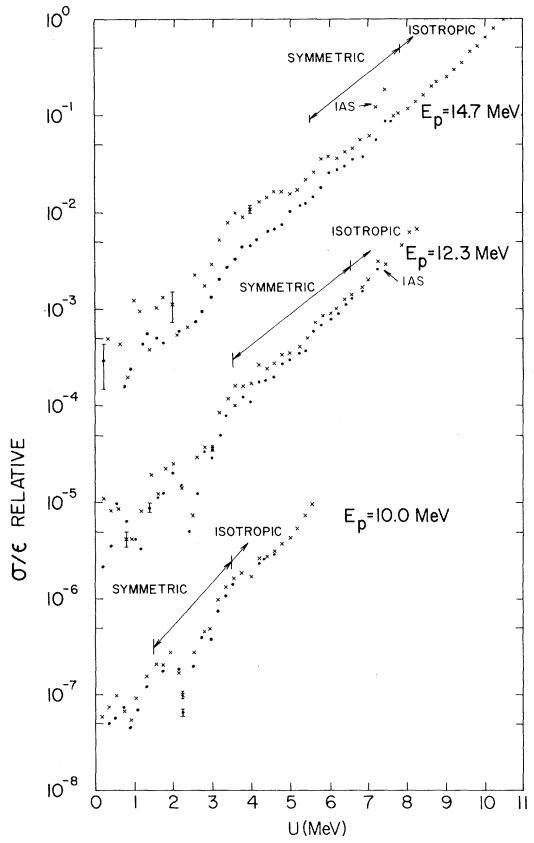

FIG. 8. Same as Fig. 6 for the ^{59}Co$(p, n)^{59}$Ni reaction.

obtained for ^{51}Cr(1.12 MeV) and ^{59}Ni(1.05 MeV) in the $3 \leq U \leq 9$-MeV region. The difference in energy resolution between the high- and low-energy spectra is evident but the agreement in average slope between the various spectra can still be observed. The universal shape observed in Figs. 9 and 10 indicates that the (p, n) and (α, n) reaction mechanisms are almost completely compound nuclear in this energy region.

At higher energies the spectra showed behavior less consistent with the predictions of the compound-nuclear model. As indicated in Table I, the discrepancies show up first at forward angles, but as the bombarding energy is increased they appear in the backward direction as well. The 14.7-MeV (p, n) spectra (Figs. 6 and 8) and 22.7-MeV (α, n) spectra (Figs. 5 and 7) illustrate the spectral shapes obtained at higher energies. In some cases, the spectra could be fit with a constant-temperature form for the level density, but the parameters for the fit were not consistent with those obtained for the same excitation energies in the residual nucleus from spectra corresponding to lower bom-

TABLE I. Nuclear temperature as a function of E_b and U.

E_p or E_α (MeV)	U range (MeV)	T (MeV) 15°	45°	75°	105°	135°
		^{51}V$(p,n)^{51}$Cr				
10.0	3–5	1.12	1.07	1.09	1.11	1.05
10.7	3–6	1.16	1.12	1.15	1.13	1.09
12.3	3–6	1.42	1.43	1.39	1.34	1.32
	6–7	1.15	1.17	1.15	1.10	1.11
13.2	3–6	1.65	1.56	1.39	1.31	1.33
	6–9	1.19	1.17	1.15	1.19	1.11
14.7	3–6	1.84	1.79	1.80	1.63	1.55
	6–9	1.70	1.48	1.50	1.55	1.38
	9–10	1.12	1.06	1.04	1.07	1.05
		^{48}Ti$(\alpha,n)^{51}$Cr				
12.2	3–5	1.14	1.04	1.08	1.06	1.06
14.0	3–6	1.21	1.13	1.14	1.12	1.11
	6–8	1.15	1.08	1.09	1.07	1.09
16.0	3–6	1.81	1.73	1.49	1.52	1.43
	6–9	1.17	1.10	1.13	1.11	1.12
17.7	3–6	2.56	1.80	1.57	1.61	1.57
	6–9	1.58	1.42	1.36	1.33	1.35
20.0	3–6	3.20	2.30	2.40	1.83	1.72
	6–9	1.95	1.74	1.45	1.46	1.45
		^{59}Co$(p,n)^{59}$Ni				
10.0	3–5	1.2	1.08	1.13	1.09	1.07
10.7	3–6	1.17	1.06	1.08	1.04	1.06
12.3	3–6	1.31	1.25	1.17	1.12	1.08
	6–8	1.09	1.05	1.07	1.05	1.02
13.2	3–6	1.35	1.30	1.15	1.22	1.14
	6–9	1.17	1.15	1.13	1.14	1.09
14.7	3–6	1.63	1.46	1.46	1.29	1.26
	6–9	1.37	1.29	1.31	1.28	1.25
	9–10	1.06	1.01	1.05	1.07	1.00
		^{56}Fe$(\alpha,n)^{59}$Ni				
14.0	3–6	1.09	1.01	1.03	1.05	1.01
16.0	3–6	1.25	1.18	1.13	1.07	1.04
	6–7	1.18	1.10	1.07	1.03	1.06
17.7	3–6	1.39	1.28	1.12	1.04	1.09
	6–9	1.23	1.17	1.09	1.10	1.04
20.0	3–6	1.92	1.64	1.39	1.29	1.24
	6–9	1.56	1.41	1.28	1.23	1.25

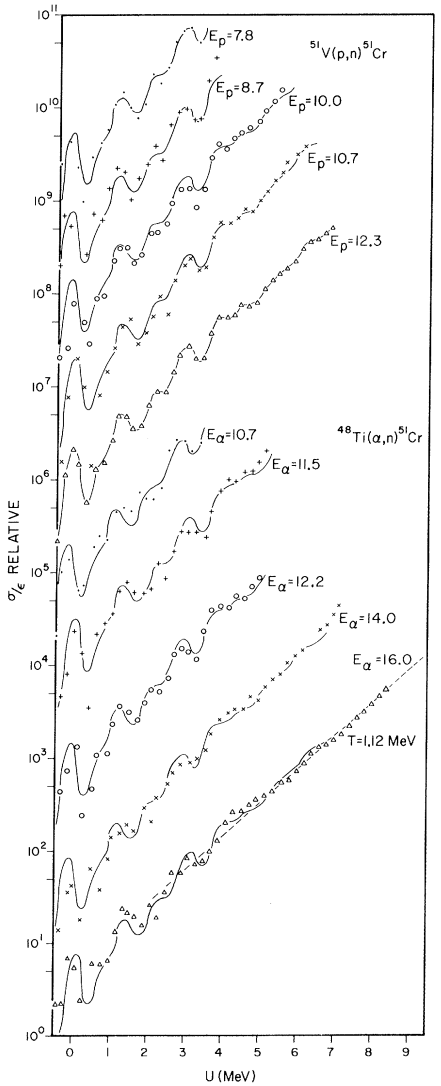

FIG. 9. Comparison of 135° neutron spectra produced in the ^{51}V$(p, n)^{51}$Cr and ^{48}Ti$(\alpha, n)^{51}$Cr reactions. The solid line was obtained by connecting the data points in the 12.3-MeV ^{51}V$(p, n)^{51}$Cr spectrum. Indicated on the 16-MeV ^{48}Ti$(\alpha, n)^{51}$Cr spectrum is the straight line corresponding to the best-fit value of the nuclear temperature ($T = 1.12$ MeV) in the region $3 \leq U \leq 9$ MeV.

barding energies. No fit for any value of the temperature with the constant-temperature form of the level density could be obtained for other spectra. The discrepancies were always caused by an excess of high-energy neutrons, which led either to a higher value for the temperature or a curving of the spectrum in this region such that no straight line could be fit to the data. Such deviations are in the opposite direction to those expected from a Fermi-gas dependence of temperature on excitation energy. Because such behavior contradicts the assumption that the level-density parameters depend only on residual excitation, it is clear that some noncompound-nuclear processes must be involved. An analysis of these contributions is presented in Sec. III B.

Equation (3) can be used to extract the moment of inertia from the observed anisotropies in the energy regions where the neutrons are produced by compound-nuclear reactions. If σ is expressed in terms of the moment of inertia I of the residual nucleus, and the nuclear temperature T, the following relation obtains:

$$\eta = \mu_b E_b \mu_n E_n R^4/2(2IT/\hbar^2)^2\hbar^4$$
$$= 25\mu_b \mu_n E_b E_n/32M^2T^2\chi^2, \quad (5)$$

where M is the mass of the residual nucleus and χ is I/I_R, the ratio of the moment of inertia of the nucleus to the corresponding rigid-body moment of inertia ($\frac{2}{5}MR^2$). Thus, from the values of η as a function of E_b and E_n the moment of inertia of the residual nucleus can be obtained.

The η values for the (p, n) reaction were too small to be determined accurately and the (α, n) spectra above 17.7 MeV were not symmetric; the remaining spectra were used to calculate σ. The neutron spectra were averaged over 1-MeV intervals and the resulting angular distributions fitted with a Legendre-polynomial expansion including l values from 0 through 3. For those groups for which the $P_1(\cos\theta)$ or $P_3(\cos\theta)$ components were nonzero [chiefly, the higher-energy neutrons in the 17.7-MeV ^{48}Ti(α, n) spectra], no σ value was calculated.

Values for the moment of inertia are expressed in terms of the ratio χ of the measured to the rigid-body value in Fig. 11. Comparison of the results for various U values provides no evidence for changes in I in the range $3 \leq U \leq 9$ MeV; the measurements are not accurate enough to rule out a slow variation of I with U. For ^{51}Cr the average of the ratio I/I_R is 0.57, while for ^{59}Ni the corresponding value is 0.38.

B. Noncompound Reactions

Calculations by Griffin,[9] Blann,[10] and Williams[11] lead to predictions for the energy distribution of nucleons emitted in pre-equilibrium decays of the compound nucleus. The basic assumption of the model is that the incident particle and target nucleus interact to form a p_0 particle and h_0 hole state (where n_0, the initial exciton number, $= p_0 + h_0$). This state can decay in two ways: (1) It could decay into a p_0+1 particle and h_0+1 hole

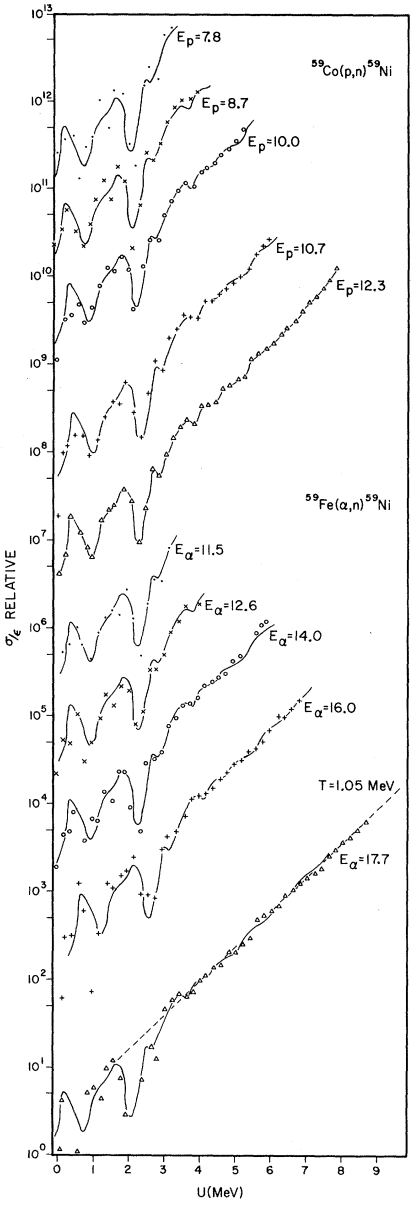

FIG. 10. Comparison of 135° neutron spectra produced in the ^{59}Co$(p, n)^{59}$Ni and ^{56}Fe$(\alpha, n)^{59}$Ni reactions. The solid line was obtained by connecting the data points in the 12.3-MeV ^{59}Co$(p, n)^{59}$Ni spectrum. Indicated on the 17.7-MeV ^{56}Fe$(\alpha, n)^{59}$Ni spectrum is the straight line corresponding to the best-fit value of the nuclear temperature ($T = 1.05$ MeV) in the region $3 \leq U \leq 9$ MeV.

state. (2) With a small probability, it could decay into a free particle and excited residual nucleus. All more complicated pre-equilibrium states have the same two possibilities for decay, with the result that the emission spectrum has both an equilibrium and a pre-equilibrium component, the latter of which will include contributions from each of the pre-equilibrium stages of the approach to equilibrium. Williams[11] shows that the pre-equilibrium spectrum has the following form:

$$\sigma(\theta, \epsilon) \propto \frac{\epsilon\sigma(\epsilon)}{(gE^*)^3} \sum_{\substack{n=n_0 \\ \Delta n=2}} \left(\frac{U}{E^*}\right)^{n-2} (n^3 - n), \qquad (6)$$

where ϵ is the channel kinetic energy, $\sigma_c(\epsilon)$ is the inverse capture cross section, g is the usual single-particle level density, and E^* is the excitation energy of the compound nucleus. The remaining parameter (n_0) is the exciton number of the first intermediate state formed. A discussion of the proper technique for determining n_0 is presented in Appendix B. Under the assumption that each transition increases the exciton number by two, the initial intermediate state would be expected to differ from the entrance-channel state by the presence of an additional particle-hole state and thus have a value for n_0 two units higher than the nucleon number of the incident projectile. A somewhat higher value for n_0 would be obtained if the first formed state cannot decay into the final state of interest. The calculations of Williams[11] tend to justify the assumption that the transition $n \to n+2$ (particle-hole creation) will be more probable than the transitions $n \to n$ (exciton scattering) or $n \to n-2$ (particle-hole annihilation).

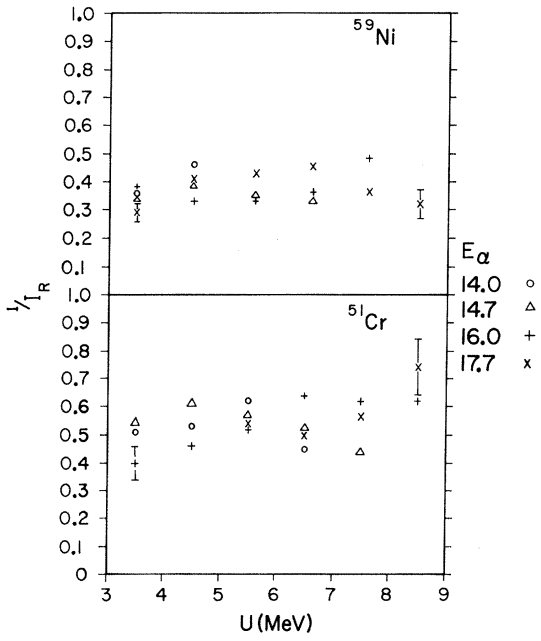

FIG. 11. The ratio of the measured moment of inertia I to the rigid-body moment of inertia for ^{51}Cr and ^{59}Ni as a function of excitation energy. The symbols ○, △, +, and × denote the data for bombarding energies of 14.0, 14.7, 16.0, and 17.7 MeV, respectively. Typical uncertainties are indicated.

At a given bombarding energy the series in Eq. (6) can be expressed in the form

$$\frac{\sigma(\theta, \epsilon)}{\epsilon\sigma_c(\epsilon)} = BU^m \left[1 + B_1\left(\frac{U}{E}\right)^2 + B_2\left(\frac{U}{E}\right)^4 + \cdots\right]. \qquad (7)$$

If $\sigma_c(\epsilon)$ is assumed to be constant, then the U dependence of $\sigma(\theta, \epsilon)/\epsilon$ should be U^m in the region $U < E$. Since, in general, equilibrium emissions will also be present in the spectrum, $\sigma(\theta, \epsilon)/\epsilon$ would be given by $A\rho(U) + BU^m$, where $\rho(U)$ is the level density of the residual nucleus. On the basis of the analysis in Sec. III A, it was concluded that the level densities for both ^{51}Cr and ^{59}Ni could be expressed in the form $e^{U/T}$, where $T = 1.05$ for ^{59}Ni and $T = 1.12$ for ^{51}Cr. Thus, if pre-equilibrium contributions are present, it would be expected that the spectrum would have the form

$$\sigma(\theta, \epsilon)/\epsilon = Ae^{U/T} + BU^m. \qquad (8)$$

Griffin[15] has pointed out that information about direct reactions can be obtained by using the same level-density formula for simple residual states as is used for the calculation of the pre-equilibrium-emission spectrum. The derivation[9-11] of the precompound energy distribution utilizes the level-density formula $\rho_n(U) \propto U^{n-1}$, where $\rho_n(U)$ is the density of n-exciton states at the excitation energy U. Because of the nature of a direct reaction, the final states of the residual nucleus reached in such a process are expected to have a simple configuration relative to the initial state. Griffin examined the dependence on residual excitation energy of a number of (α, p) spectra for odd-Z targets and demonstrated that the observed spectral shape was consistent with the predictions obtained under the assumption that the final states corresponded to four-exciton states. In the distorted-wave Born approximation (DWBA), the cross section for a direct process to a group of states f is given by

$$\sigma_D \propto (K_f/K_i)\,|V_{fi}|^2 \rho_f(U)dU, \qquad (9)$$

where K_i and K_f are the initial and final wave numbers, respectively, and V_{fi} is the matrix element connecting initial and final states. At a given bombarding energy, the spectrum should have the form $\sigma_D \propto K_f \rho_f(U)dU$. If the spectrum contains both direct and compound contributions, the form

$$\sigma(\theta,\epsilon)/\epsilon = Ae^{U/T} + C\,\rho_f(U)/\sqrt{\epsilon}$$
$$= Ae^{U/T} + C\,U^{n-1}/\sqrt{\epsilon} \qquad (10)$$

would be expected, where n is the exciton number of the residual state formed in a direct reaction. An expansion of $\sqrt{\epsilon} = (E_b + Q - U)^{1/2}$ in powers of $U/(E_b + Q)$ makes it possible to eliminate the explicit ϵ dependence of the second term and results in the following form:

$$\frac{\sigma(\theta,\epsilon)}{\epsilon} = Ae^{U/T} + C\,U^{n-1}\left[1 - \frac{U}{2(E_b+Q)} + \frac{3}{8}\left(\frac{U}{E_b+Q}\right)^2 - \cdots\right]$$
$$\simeq Ae^{U/T} + B\,U^m. \qquad (11)$$

For values of $U < E_b$, it can be seen that Eq. (11) reduces to the form of the expression given in Eq. (8). Thus, both pre-equilibrium and direct contributions to the spectrum will have the same type of dependence on U, although in general they would correspond to different m values.

The formulations of the pre-equilibrium model[9-11] have not included discussions of the angular distribution to be expected from such a reaction mechanism. No prediction for the form of the angular distribution can be made without some assumption as to the lifetime of such states. Because the theories of pre-equilibrium emission assume that such processes can be separated from direct contributions, they rest on the assumption that the lifetime of pre-equilibrium states is significantly longer than the single-particle transit time across the nucleus. In such a case the angular distribution would be symmetric about 90°, for the same reason that compound-nuclear processes have a symmetric angular distribution. This point is discussed in greater detail in the Appendix A.

The analysis was carried out by fitting each (p,n) or (α,n) spectrum with the temperature obtained in Sec. III A and various values of m. As expected, the spectra for proton energies of 12 MeV or less and those for α energies of 16 MeV or less were fit as well with just the exponential term as with the form shown in Eq. (8); this provides evidence for the correctness of the fitting procedure.

At higher energies the fitting procedure was sufficiently sensitive to show a variation in quality of fit as a function of m value. The fitting region extended from $U = 3$ MeV as the lower boundary (below which the level density was too low to apply a statistical treatment) to a maximum U for which data were available if this value was lower than 9 MeV. The upper limit of 9 MeV was selected because of the presence of $(p, 2n)$ or $(\alpha, 2n)$ neutrons beyond this region.

Typical fits for a (p,n) and (α,n) reaction are shown in Figs. 12 and 13, respectively. Table II lists the best-fit m values as a function of reaction, angle, and energy. Where more than one value is listed, the values shown provided equally good fits. An estimate of the sensitivity of the fitting procedure can be obtained from Fig. 14, which shows the fits obtained for various m values.

The value of m for the (α,n) reaction would be expected to be approximately two for the direct contribution (corresponding to a three-exciton re-

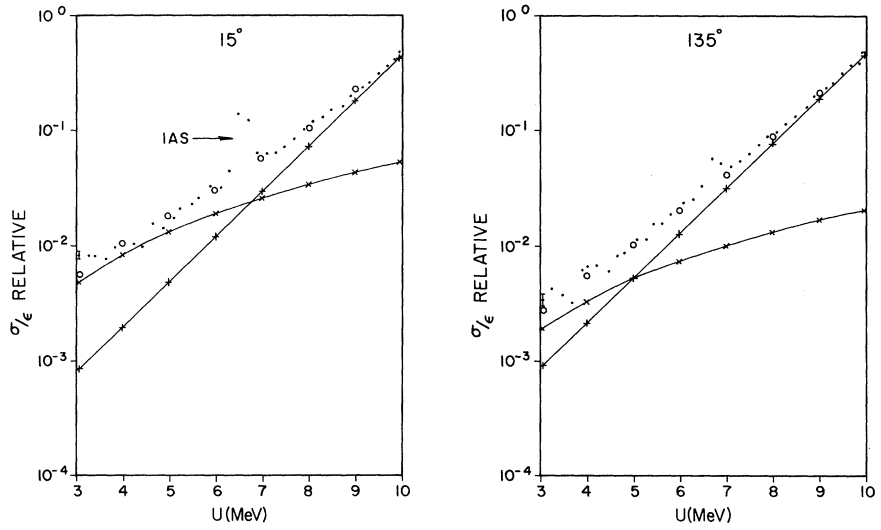

FIG. 12. Fits of the form $Ae^{U/T} + BU^m$ to the 14.7-MeV $^{51}V(p,n)^{51}Cr$ neutron spectrum. Both a forward angle (15°) and a backward angle (135°) are shown. The experimental spectrum is denoted with ●, the $Ae^{U/T}$ term contribution (compound) with +, the BU^m contribution (noncompound) with ×, and the sum $Ae^{U/T} + BU^m$ with ○.

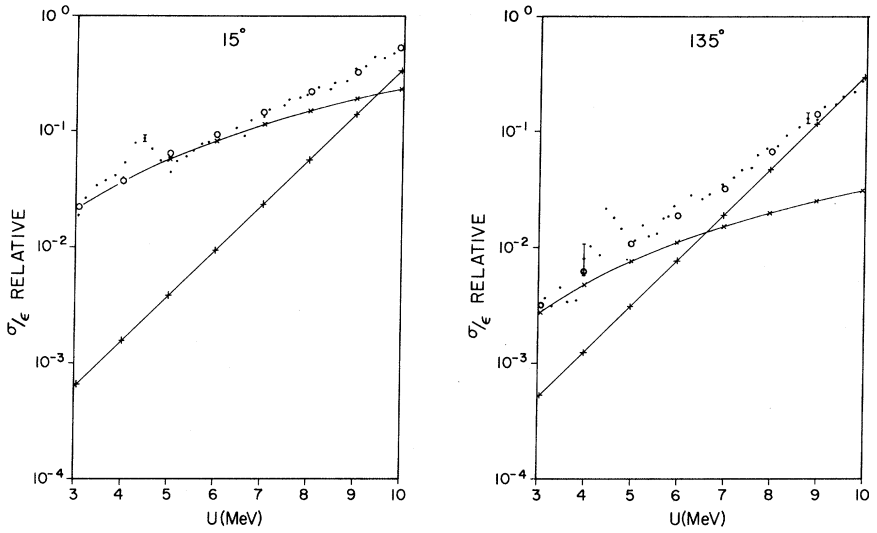

FIG. 13. Same as Fig. 12 for the 22.7-MeV ^{48}Ti(α, n)-^{51}Cr reaction.

sidual state) and four or higher for a pre-equilibrium contribution (corresponding to a six-exciton intermediate state). The values shown in Table II provide some evidence for pre-equilibrium contributions at 16 MeV, but these are overwhelmed at higher energies by a substantial direct contribution.

Either a direct or a pre-equilibrium (p, n) reaction would probably yield a value of 1 for m, because in both cases it is expected that the residual states will be one-particle (proton) and one-hole (neutron) states. In fact, the observed best-fit m values are somewhat higher. This is probably a consequence of the fact that the fits were made in the region $3 \leq U \leq 9$; a smaller value for m might be obtained if a fit could be performed for smaller U/E^* values. The energy distribution for either a direct or a pre-equilibrium reaction would also contain terms of higher order in U and a fit including regions where U is not small compared to E^* might show the effects of these terms.

More information on the reaction mechanisms involved can be obtained by examining the dependence of B on both angle and bombarding energy. As can be seen from Eq. (6), the dependence on bombarding energy of the first term in the expression for the pre-equilibrium spectrum $\sigma(\theta, \epsilon)/\epsilon$ is $1/(E^*)^{n+1}$, where E^* is the excitation energy in the compound nucleus and n is the exciton number of the intermediate state involved. For a direct reaction, the dependence of $\sigma(\theta, \epsilon)/\epsilon$ on bombarding energy is indirect and comes about through the variation of $|V_{fi}|^2$ with energy. This is a function of the nuclear potential and cannot be evaluated without specifying the potential, but would be expected to be approximately $1/E_b$ or $1/E_b^2$, i.e., the cross section is assumed approximately constant or varying as $1/E_b$.

In Fig. 15 is shown the bombarding- and excitation-energy dependence of the parameter B for both the (α, n) and (p, n) reactions. Also indicated (with dashed lines) is the energy dependence expected for pre-equilibrium and direct reactions.

TABLE II. Best fit m values.

E_p or E_α (MeV)	15°	45°	75°	105°	135°
			^{51}V(p,n)^{51}Cr		
12.3	1	0	2	a	a
13.2	1	2	1,2	2,3	2
14.7	1,2	2	2,3	2	3
			^{48}Ti(α,n)^{51}Cr		
16.0	2	3	3,4	a	a
17.7	2	2,3	2	3	3,4
20.0	1,2	2	1,2	2,3	2
22.7	2	3	2	2,3	3
			^{59}Co(p,n)^{59}Ni		
12.3	1	2	1,2	a	a
13.2	2	3	2	2	1,2
14.7	2	1,2	3	1,2	2
			^{56}Fe(α,n)^{59}Ni		
16.0	3	5	a	a	a
17.7	2	2,3	2	3,4	a
20.0	1,2	2	3	2,3	4,5
22.7	2	3	2,3	2	2,3

[a]Spectra were fit so well with the exponential term that no value for m could be obtained.

The limited energy range for which data are available and the magnitude of the errors on the $B(E, \theta)$ values make it impossible to rule out either process on the basis of the energy dependence of this part of the cross section. The differences between the expected behavior for direct reactions and that for pre-equilibrium reactions make it possible to use the variation with energy to distinguish between the two processes, but clearly data must be available over a large energy range.

The angular dependence of the $B(E, \theta)$ values is also useful in identifying the reaction mechanism involved. As can be seen in Fig. 16, the contribution to the spectrum represented by the B values is strongly forward peaked for the (α, n) reaction, suggesting that the reaction mechanism involved is direct. Also shown for comparison is the angular dependence predicted for a direct (α, n) reaction with the relation $\sigma(\theta) \propto 1/(kR)^2$, which can be obtained semiclassically by assuming that the reaction occurs at the surface of the nucleus and that the presence of many different l-transfer contributions will obliterate the diffraction minima and maxima. Considering the crudeness of the calculation, the agreement between the measured and calculated values is quite good.

Figure 16 also shows the angular dependence of the B values obtained from the (p, n) reaction. The shape of this portion of the spectrum is not as strongly forward peaked as would be expected from $1/(kR)^2$ nor is it symmetric (for a pre-equilibrium reaction). Shown for comparison in Fig. 16 is the angular distribution for the (p, n) reaction to the analog state, a reaction known to be direct. In this case, as was observed for the energy dependence of the cross section, the behavior of the noncompound component of the (p, n) reaction is between the predictions for direct- and pre-equilibrium-reaction mechanisms.

C. Extension of Level-Density Measurements Beyond 9 MeV

The procedure discussed in Sec. III A cannot give reliable values for the level densities of ^{51}Cr and ^{59}Ni beyond 9 MeV, because of the presence of $(p, 2n)$ and $(\alpha, 2n)$ neutrons in this region. An alternative technique, suggested by Ericson,[16] can be utilized to extend the level-density measurements beyond this point. For a reaction which proceeds to a given final state through a compound

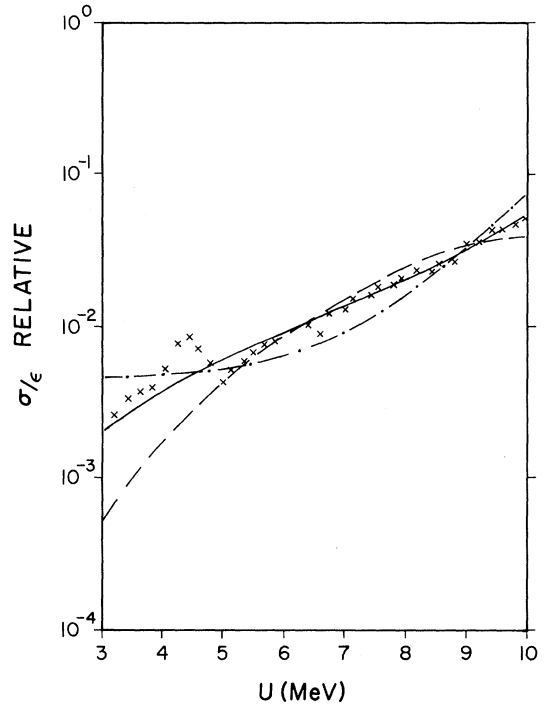

FIG. 14. Variation of the quality of fit to the neutron spectrum of the expression $Ae^{U/T} + BU^m$ as a function of m. The 22.7-MeV ^{48}Ti$(\alpha, n)^{51}$Cr spectrum at 15° is the example shown. The experimental spectrum is denoted by ×, and the best-fit spectra for $m = 0$, 2, and 4 are denoted by the dot-dash line, the solid line, and the dashed line, respectively.

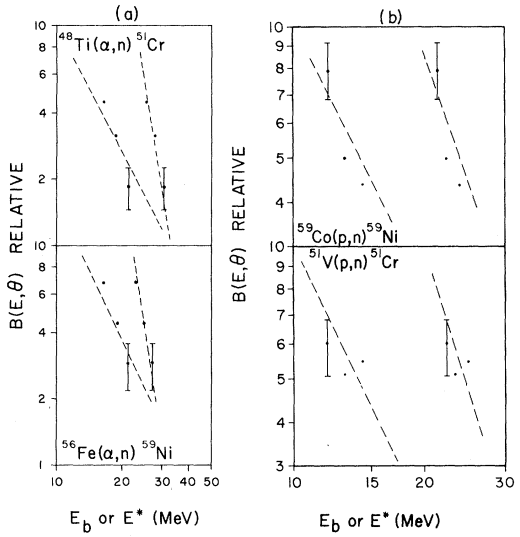

FIG. 15. Dependence of $B(E, \theta)$ on both the bombarding energy (E_b) and excitation energy in the compound nucleus (E^*). On the left for each reaction (a) and (b) is the plot against E_b; the dashed line is the approximate bombarding energy dependence $(1/E_b{}^2)$ expected for σ/ϵ from a direct reaction. The corresponding points on the right show the variation of $B(E, \theta)$ with E^*; the dashed line is the excitation energy dependence expected for a pre-equilibrium reaction $[(1/E^*)^7$ for (α, n), $(1/E^*)^4$ for $(p, n)]$. (a) The ^{48}Ti$(\alpha, n)^{51}$Cr and ^{56}Fe(α, n)-^{59}Ni reactions. (b) The ^{51}V$(p, n)^{51}$Cr and ^{59}Co$(p, n)^{59}$Ni reactions.

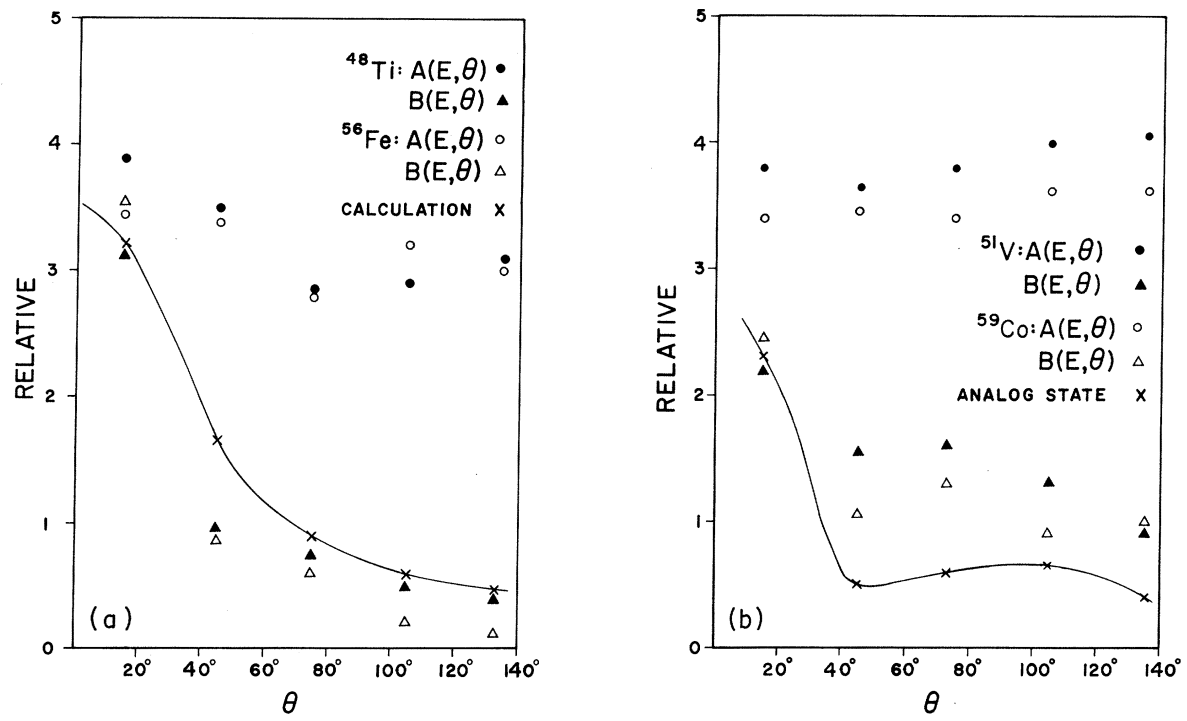

FIG. 16. Dependence of $A(E,\theta)$ and $B(E,\theta)$ on θ. (a) The ^{48}Ti$(\alpha,n)^{51}$Cr and ^{56}Fe$(\alpha,n)^{59}$Ni reactions for $E\alpha = 22.7$ MeV. The points labeled x denote the expected angular dependence for a direct reaction calculated from the assumption of a black nucleus. (b) The ^{51}V$(p,n)^{51}$Cr and ^{59}Co$(p,n)^{59}$Ni reactions for $E_p = 14.7$ MeV. The points labeled × denote the angular distribution obtained for the isobaric analog state in the ^{51}V$(p,n)^{51}$Cr reaction at 14.7 MeV.

nucleus, the energy dependence of the cross section is determined primarily by the level densities in the residual nuclei. If the effects due to changes in transmission coefficients can be either ignored or corrected for, the decrease in $\sigma(\epsilon)$ to a particular final level will be determined by the rate of increase of the levels accessible in the residual nuclei. The Coulomb barrier will inhibit competition due to residual nuclei reached in charged-particle emission so that the rate of change of the cross section will be determined primarily by the level density in the residual nucleus reached by neutron emission.

This can be put on a more quantitative basis with the use of Eq. (1).

$$\sigma(\epsilon) \propto \epsilon\, \sigma_c(\epsilon)\, \rho(U)\,. \tag{12}$$

If it is assumed that σ_c is constant and that all channels can be ignored except the neutron channel, the following expression is obtained:

$$\sigma_{\text{abs}}(E_b) = \int \sigma(\epsilon) d\epsilon = k \int \epsilon\, \rho(E-\epsilon) d\epsilon\,, \tag{13}$$

where σ_{abs} is the total absorption cross section. Thus,

$$\sigma(\epsilon)/\epsilon = \sigma_{\text{abs}}(E_b) \Big/ \int \epsilon\, \rho(E-\epsilon) d\epsilon \tag{14}$$

for one level. The technique of analysis described in Sec. III B involved determining the fraction of the emission spectrum for $3 \leq U \leq 9$ MeV which was due to compound-nuclear reactions at various bombarding energies. This means that instead of one level as in Eq. (14), one is summing over all levels between 3 and 9 MeV. In this case the following relation is obtained:

$$A(E_b) \propto \sum_{3 \leq U \leq 9\ \text{Mev}} \frac{\sigma(\epsilon)}{\epsilon}$$

$$\propto \frac{\sigma_{\text{abs}}(E_b)}{\int_0^{U_M} (E-U) e^{U/T} dU} \propto \frac{\sigma_{\text{abs}}(E_b)}{T^2 \rho(U_M)}\,, \tag{15}$$

where $U_M (= E_{\text{c.m.}} + Q)$ is the maximum possible residual excitation energy at the bombarding energy E_b. The proton absorption cross sections were calculated with the optical-model parameters of Hodgson,[17] while the corresponding α parameters were those proposed by Benveniste, Merkel, and Mitchell.[18] Use of the $A(E_b)$ values for low bombarding energies gave relative values for the level density in the region below 9 MeV; these were used to normalize the relative points obtained from this technique to the values obtained from analysis of the spectral shape. The resultant

curves are shown in Figs. 17 and 18 and indicate that the constant-temperature level-density form remains appropriate considerably beyond $U = 9$ MeV. The deviations from the constant-temperature form are in a direction consistent with the expected transition to Fermi-gas behavior as the energy is increased.

The general form for the contribution of each level to a continuum spectrum[19] indicates that the weighting of each residual level in an emission spectrum is proportional to $(2J+1)$. Thus, the relation between the spectrum and the level density is actually

$$\sigma(\epsilon) \propto \epsilon\, \sigma_c(\epsilon) \sum_J (2J+1)\, \rho(U, J) \propto \epsilon\, \sigma_c(\epsilon) \langle 2J+1 \rangle \rho(U), \tag{16}$$

where $\langle 2J+1 \rangle$ is the expectation value of $2J+1$ at the energy U. If the usual dependence of $\rho(U, J)$ on J is assumed, $[\rho(U, J) \propto (2J+1) e^{-J(J+1)/2\sigma^2}]$, $\langle 2J+1 \rangle$ can be shown to be $(2\pi\sigma^2)^{1/2}$; for the case in which σ is constant or slowly varying, the presence of this factor can be ignored, as is usually done. The normalization of such a relative level-density measurement cannot be carried out against an absolute level-density count in regions where levels can be resolved, but must be compared with a normalized level count in which each level is weighted by the factor $(2J+1)/\langle 2J+1 \rangle$. Because the J values are not known for all low-lying levels for ^{51}Cr and ^{59}Ni, such a normalization could not be made.

Instead, the normalization was carried out with the use of the absolute cross section to the ground state for the ^{51}V$(p, n)^{51}$Cr reaction and the first three levels for the ^{59}Co$(p, n)^{59}$Ni reaction at $E_p = 7.8$ MeV. If spin effects are included in Eq. (14), the cross section $\sigma(\epsilon)$ to a particular final level of spin J for an outgoing neutron energy of ϵ is

$$\frac{\sigma(\epsilon)}{\epsilon} = \frac{\sigma_{\text{abs}}(2J+1)}{\langle 2J+1 \rangle \int_0^{U_M} (U_M - U)\rho(U)\, dU} = \frac{\sigma_{\text{abs}}(2J+1)}{(2\pi\sigma^2)^{1/2} T^2 K e^{U_M/T}}, \tag{17}$$

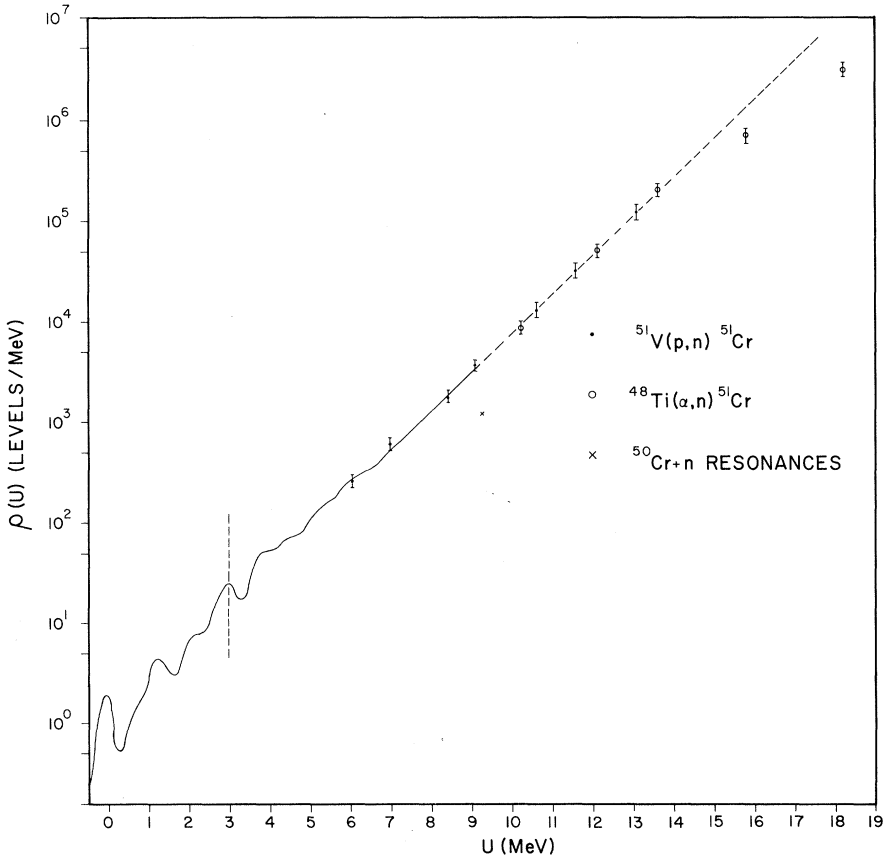

FIG. 17. Level density of ^{51}Cr between $U = 3$ MeV and $U = 18$ MeV. The solid line is the curve obtained from Fig. 9; the extension of the level density beyond 9 MeV and the absolute normalization (carried out for the point near 6 MeV) are based on the analysis described in Sec. III C. The dashed line indicates approximately the point below which the differential spectrum is no longer proportional to the level density.

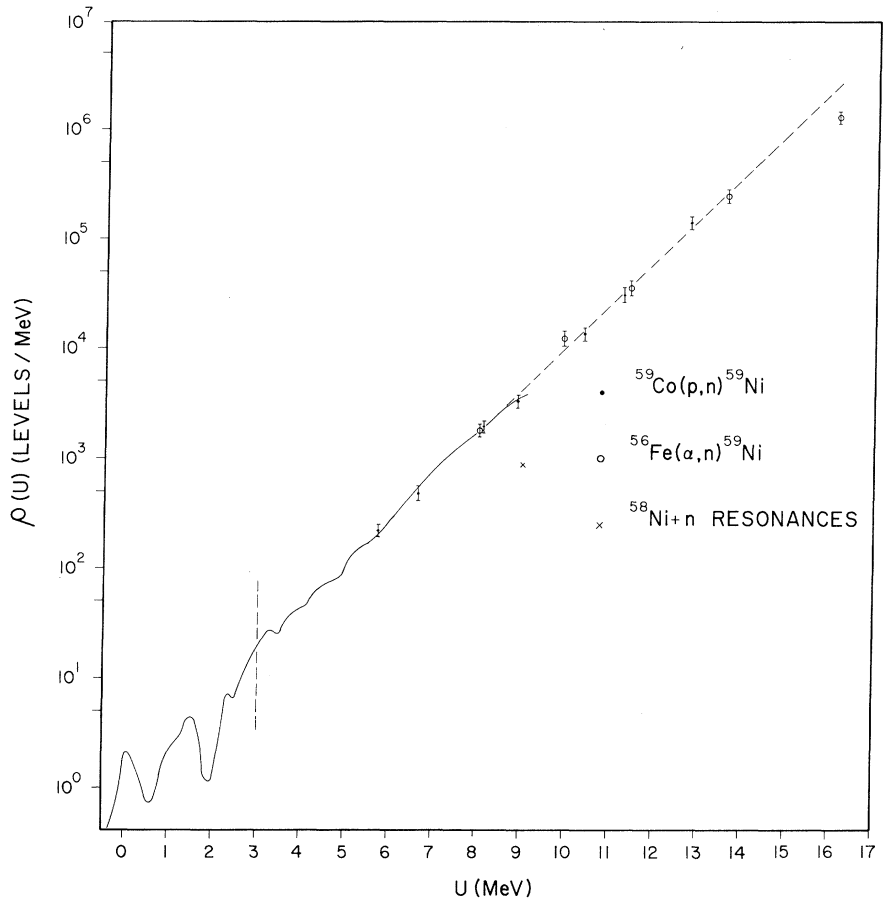

FIG. 18. Same as Fig. 17 for ^{59}Ni; the solid line is obtained from Fig. 10.

where $\langle 2J+1\rangle$ is the expectation value of $2J+1$ averaged over J and U, and $\rho(U)$ has been replaced by $Ke^{U/T}$. σ values are obtained from the analysis in Sec. III A.

The computer code LOKI calculated the reaction cross sections for ^{51}V and ^{59}Co with the potential parameters of Hodgson; these had to be corrected for the effects of (1) direct inelastic processes [primarily (p,p') to collective states], (2) preequilibrium emissions, and (3) the component of the cross section for which the isospin T is $T_0+\frac{1}{2}$. A rough estimate of the combined magnitude of these corrections is 25%. Since all of these effects tend to enhance the (p,p') cross section at the expense of the (p,n), the correctness of this estimate can be gauged by comparing the cross sections $\sigma(p,n)$ and $\sigma(p,p')$. According to Hansen and Albert,[20] the ratio $\sigma(p,p')/\sigma(p,n)$ is about 1:3; thus the approximate estimate listed above is not inconsistent with experiment. The corrected $\sigma_{abs}(=0.75\times\sigma_{reaction})$ was substituted in Eq. (17) to provide an absolute level density at about 6 MeV. Also shown on the plot are the level densities for ^{51}Cr and ^{59}Ni at the neutron binding energy; these were obtained from the density of $\frac{1}{2}^+$ levels measured by Bilpuch *et al.*[21] and the value of $2\sigma^2$ extracted from the analysis described in Sec. III A. Equation (3) is obtained by Ericson and Strutinski with the use of the sharp-cut off approximation. The values for $2\sigma^2$ for ^{51}Cr and ^{59}Ni were evaluated using the expectation values for the angular momenta calculated from the transmission coefficients for the potentials of Hodgson (neutrons) and Benveniste (α particles) rather than the sharp-cutoff values producing an increase of 25% in the values of σ obtained. The agreement between the neutron-resonance values and the present measurements is poor; the lack of agreement will be discussed in Sec. IV.

IV. DISCUSSION

A. Level Densities

Recent measurements of the excitation-energy dependence and absolute magnitude of level-density functions for nuclei in the same mass region as those measured in the present experiment include those of Fluss *et al.*[22] and Huizenga *et al.*[23] The proton and α spectra produced by the $\alpha+^{56}$Fe and $p+^{59}$Co systems were studied in the first experi-

ment; the residual nuclei ^{56}Fe and ^{59}Co were found to have constant-temperature level densities with temperatures about 1.2 MeV. The results of the present experiment indicate that there is some possibility of direct and pre-equilibrium contributions in the continuum spectra at the energy used by Fluss *et al.*; nonetheless, the constant-temperature form and the values of T obtained are in reasonably good agreement with the present measurements for nuclei in this mass region.

Huizenga *et al.* utilized the cross sections of the ^{56}Fe$(\alpha, p)^{59}$Co and ^{59}Co$(p, \alpha)^{56}$Fe reactions to low-lying residual states to obtain absolute level-density measurements for the residual nuclei ^{56}Fe, ^{59}Co, and ^{59}Ni. Their data can be fit with either a back-shifted Fermi gas or a constant-temperature level density, but the agreement with the present measurements is poor because the value of T obtained by Huizenga *et al.* was 1.5 MeV. This value for T is sufficiently high that the cross sections proceeding through the compound nucleus ^{60}Ni would depend on the level densities of ^{56}Fe and ^{59}Co, as well as ^{59}Ni, while the temperatures obtained in the present experiment are so low that the cross sections would depend essentially only on the level density of ^{59}Ni.

The present technique for determining relative level densities from absolute cross sections in the continuum has two important advantages over the technique used by Huizenga *et al.*, which uses the cross section to a single level. Because the cross sections to be measured are in the continuum, their magnitudes are much larger than those to individual levels and counting statistics become an insignificant source of error. In addition, the shape of the spectrum can be determined at lower energies making possible the subtraction of non-compound contributions at higher energies, where the single-level technique would be difficult if not impossible to use. If, as proposed in Appendix A, pre-equilibrium contributions to a cross section also result in a symmetric angular distribution, the traditional criterion of symmetry about 90° as a sufficient condition for a compound-nuclear reaction may be invalid. As can be seen from the formulas in Sec. III B, the contributions of pre-equilibrium and direct processes relative to compound processes are larger for small values of U; this region is precisely where the cross sections to isolated levels can be measured.

The absolute cross sections to low-lying levels obtained in the present experiment are not as inconsistent with those of Huizenga *et al.* as might be inferred from the differences in the level densities obtained from the two sets of data.

As can be seen from Eq. (15), the absolute cross section to a particular final level is determined by the competition with all other decay channels. One deduces a level density from this competition, i.e., the competition is given by $\int_0^{U_M}(U_M - U)\rho(U)dU$, which will be $T^2\rho(U_M)$ if $\rho(U) = Ke^{U/T}$. Since the values for this integral measured in the two experiments agree to within 20% below $U = 9$ MeV, the differences in deduced level densities arise from the different temperatures used.

The most important sources of error in the continuum cross section are those due to the error in the absolute value of the cross section due to detector efficiency and the uncertainty of the energy scale. An uncertainty of ΔE in the bombarding energy produces an essentially identical uncertainty in the residual excitation; this would make the level-density measurement incorrect by a factor $e^{\Delta E/T}$. Smaller contributions to the error result from the relative uncertainty of the absorption-cross-section values at various energies, and the uncertainties introduced by the fitting procedure. The combined effects of these errors is to make the relative level-density determination uncertain by 15%.

The error on the absolute level density is substantially larger, primarily because of the uncertainties in σ, the spin-cut-off parameter, and σ_{abs}, the absorption cross section. The values for σ were obtained from analysis of the anisotropy of the angular distributions for the (α, n) reaction.

As was explained in Sec. III C, the values $\langle I_b^2\rangle$ and $\langle I_n^2\rangle$ were evaluated using partial cross sections as functions of J calculated from optical parameters. It is felt that uncertainties in these parameters could result in a 10% error in σ; this would change the absolute normalization by the same factor, but more importantly, would change the value obtained by resonance counting at the neutron binding energy by twice this amount, since this value is proportional to σ^2. The absorption cross section and the corrections to this number for direct reactions, pre-equilibrium emissions, and isospin effects cause an additional error in the absolute level densities of about 15%. To these errors must be added the uncertainties responsible for the relative errors as described previously, with the result that the value for the combined uncertainties introduced in the absolute level density is approximately 30%.

The measured level density at the neutron binding energy is also subject to uncertainties. As has already been pointed out, a substantial error arises from the factor of $2\sigma^2$ which converts the density of $\frac{1}{2}^+$ levels to the total level density. In addition, because the value for density of $\frac{1}{2}^+$ levels is obtained from counting a small number of levels, level statistics introduce an additional 20% uncertainty. Comparison of the measured level-width

distribution with a Porter-Thomas distribution indicates that a similar fraction of levels (those with narrow widths) may have been missed in the neutron scattering experiment. Thus, both the present measurement and the level density determined from a count of neutron-binding-energy resonances are subject to appreciable errors, but it does not seem as if the errors are large enough to explain the factor-of-3 discrepancies observed for both ^{51}Cr and ^{59}Ni.

The present measurements could be brought into agreement with the neutron-binding-energy-resonance count if the rigid-body value for σ were used. Ericson[24] compared the level densities obtained from charged-particle spectroscopy with those calculated from neutron-binding-energy-resonance counts for a number of nuclei in this mass region and concluded that a rigid-body magnitude for σ was required to bring the two level densities into agreement. However, the values of σ measured in the present experiment (Sec. III A) exclude this resolution of the discrepancy.

B. Reaction Mechanisms

The results of Sec. III B indicate that the (p, n) and (α, n) spectra at higher energies can be decomposed into a compound and a noncompound portion. On the basis of the residual-excitation-energy dependence and angular distribution it was concluded that the noncompound component was essentially direct in the (α, n) case, while for the (p, n) reaction the characteristics of this portion of the spectrum were consistent with those expected from a mixture of direct and pre-equilibrium contributions.

For the (p, n) reaction the two reaction mechanisms are difficult to separate experimentally. It is expected that a direct (p, n) reaction would populate one-particle (proton) and one-hole (neutron) states in the residual nucleus; these same states would also be populated by a pre-equilibrium process proceeding through a three-exciton intermediate state. In the continuum both mechanisms would be expected to pick out the two-exciton component of residual states, leading to an identical dependence on the residual excitation U. The present separation between the two mechanisms is not entirely conclusive, because it is based on the less definitive angular and bombarding-energy dependence.

A corresponding analysis is simpler for the (α, n) reaction. Direct stripping processes would be expected to lead to three-exciton residual states. If the pre-equilibrium process is assumed to take place as the result of a number of two-body interactions, it might be argued that in order to transfer a large fraction of the energy of the α particle (shared initially by four nucleons) to the neutron, two or three two-body interactions might be necessary, resulting in a six- or eight-exciton intermediate state. Thus, the U dependence would distinguish between the direct and pre-equilibrium components. As the exciton number n of the last intermediate state before emission is increased, the cross section for pre-equilibrium emission decreases as $U^{n-2}/(E^*)^{n+1}$, so for large n the cross section becomes quite small. A reaction such as (α, α') or $(\alpha, 3pn)$, which could occur with just one two-body interaction, would be more likely to have a large pre-equilibrium amplitude, relative to the direct and compound contributions. Another consequence of the high n value needed for an (α, n) pre-equilibrium emission is that the resultant emission spectrum will not differ appreciably in shape from the equilibrium form, making separation of such contributions difficult.

These predictions can be compared with the measurements of Blann and Lanzafame[12] of cross sections for α-induced reactions on ^{51}V. They find that the excitation functions for $(\alpha, 3n)$ and $(\alpha, p3n)$ can be fit very well with a calculated pre-equilibrium cross section above 40 MeV, but that the calculated pre-equilibrium (α, n) cross section has the wrong energy dependence. This could be a consequence of the fact that the pre-equilibrium (α, n) component is so small that the direct amplitude provides most of the cross section. This interpretation is consistent with the fact that the (α, n) cross section is an order of magnitude smaller than the $(\alpha, 3np)$ cross sections.

C. Intermediate Level Width

Because the Griffin formulation of pre-equilibrium emission neglects interference with the incident beam, its validity rests implicitly on the assumption that the lifetime of intermediate states is considerably longer than the single-particle transit time. As is shown in Appendix A, an estimate of the lifetime of a three-exciton state can be obtained from the value of the cross section for pre-equilibrium emission in the (p, n) reaction. From Eq. (A6) the pre-equilibrium cross section has the value

$$\sigma_{pe} = \sigma_{abs}\, \mu_n \sigma_c \rho_2(U)/\pi^2\hbar^2\rho_3(E^*)\Gamma_3 , \qquad (18)$$

where Γ_3 is the width of a three-exciton state. The analysis or Sec. III B provides values for the noncompound contribution in the form

$$(\sigma/\epsilon)_{\text{noncompound}} = BU .$$

The noncompound cross section for the (p, n) reaction is estimated to contain equal contributions from direct and pre-equilibrium contributions;

therefore

$$(\sigma/\epsilon)_{pe} = (4\pi B/2)U = \sigma_{abs}\mu_n\sigma_c\rho_2(U)/\pi^2\hbar^2\rho_3(E^*)\Gamma_3, \tag{19}$$

or

$$\Gamma_3 = \mu_n\sigma_{abs}\sigma_c\rho_2(U)/2\pi^3\hbar^2\rho_3(E^*)BU. \tag{20}$$

Values of 5 for g (density of single-particle states per MeV) and 1 b for σ_{abs} and σ_c were assumed. The resultant Γ_3 obtained from an average of B at 14.7 MeV for ^{59}Co$(p,n)^{59}$Ni and ^{51}V$(p,n)^{51}$Cr is 160 keV. This value is subject to large uncertainties, primarily because of the difficulty in determining the fraction of the noncompound cross section attributable to pre-equilibrium emissions, but it does have a magnitude consistent with the assumptions $\Gamma_{sp} \gg \Gamma_{int} \gg \Gamma_{CN}$ made in calculating the pre-equilibrium spectrum and should be accurate to within a factor of 2.

V. SUMMARY

An analysis of the continuum neutron spectra produced from the ^{52}Cr and ^{60}Ni compound systems has yielded information on both the level densities of ^{51}Cr and ^{59}Ni and on the reaction mechanisms involved in the (p,n) and (α,n) reactions in the 8- to 23-MeV range. For proton energies of 10 MeV or less and α energies of 14 MeV or less both reactions are essentially compound nuclear. In this range the level-density form for ^{51}Cr and ^{59}Ni can be extracted; a constant-temperature form was found to be appropriate for both nuclei.

At higher energies the spectra were resolved into compound and noncompound portions. Use of the bombarding-energy dependence of the compound portion enabled the level-density measurements to be extended to residual energies of 18 MeV; the constant-temperature form remained valid up to 14 MeV.

Examination of the noncompound contribution led to the conclusion that the (α,n) noncompound portion was essentially direct, while the corresponding (p,n) component was due to both direct and pre-equilibrium processes. The difference between the relative importance of pre-equilibrium contributions in the two reactions is that the (α,n) reaction proceeds through a higher-order process, i.e., a larger number of two-body interactions is necessary for (α,n) decay.

A study of nuclei with lower nuclear temperatures would be particularly interesting, since these nuclei should have smaller equilibrium cross sections in the energy region where pre-equilibrium cross sections are large. This result cannot be achieved by simply increasing the bombarding energy for the nuclei studied in the present experiment because, compared with the pre-equilibrium cross section, the relative decrease of the compound contribution is nullified by a relative increase of the direct contribution with increasing energy.

A relation between the pre-equilibrium cross section and the width of the corresponding intermediate state was derived. Use of the experimental values for these cross sections yielded a value for the intermediate-state width of 160 ± 80 keV. This value is consistent with the relation $\Gamma_{sp} \gg \Gamma_{int}$ and thus affirms one of the basic assumptions of the Griffin model. In addition, it satisfies the condition necessary to obtain a symmetric angular distribution from pre-equilibrium emissions.

ACKNOWLEDGMENTS

It is a pleasure to acknowledge the many helpful comments of Professor A. K. Kerman regarding the interpretation of these data.

APPENDIX

A. Lifetimes of Intermediate States

Relatively little attention has been devoted to one of the basic assumptions of the intermediate-structure calculations as applied to statistical processes. Since the pre-equilibrium calculations do not include the effects of interference with the incident beam, they will not be correct if the lifetime of an intermediate state is not substantially longer than a single-particle-state lifetime.

Neither experiment nor theory can provide conclusive indication of the correctness of such an assumption at the present time. From a theoretical standpoint, Williams[11] has shown that for an n-exciton state the transition rates to $n-2$-, n-, and $n+2$-exciton states are, respectively,

$$\lambda^- = \frac{2\pi}{\hbar}|M|^2 g\left[\frac{n^2(n-2)}{4}\right], \tag{A1}$$

$$\lambda^0 = \frac{2\pi}{\hbar}|M|^2 g^2 E^*\left(\frac{3n-2}{4}\right), \tag{A2}$$

$$\lambda^+ = \frac{2\pi}{\hbar}|M|^2\frac{g^3E^{*2}}{(n+1)}, \tag{A3}$$

where g is the single-particle level density and E^* is the excitation energy. As can be seen from these relations, $\lambda^+ \gg \lambda^0 \gg \lambda^-$ if $n \ll gE^*$. Thus, the total width of an n-exciton intermediate state can be approximated by the width for decay into $n+2$-exciton states if n is small. If it is assumed that the matrix element M^2 is the same for transitions from single-particle states to $n=3$ bound states as it is for transitions between $n=3$ and $n=5$ states, the ratio $\lambda^+_{n=3}/\lambda^+_{n=1} = \Gamma^+_{n=3}/\Gamma^+_{n=1}$ can be

shown to be $\frac{1}{2}$. This substantially underestimates Γ_{sp}, however, since it neglects the width of the single-particle state to the continuum. If this is assumed to be equal to the width for decay into a three-exciton state, the ratio would be $\Gamma_{n=3}/\Gamma_{sp} \sim \frac{1}{4}$. Because of the difficulties in estimating the relative fractions of the single-particle width to the continuum and to the $n=3$ states and because the matrix element connecting the single-particle states to the bound states may be different from that connecting $n=3$ to $n=5$ states, this estimate is subject to large uncertainties.

Since $\Gamma_n = \hbar\lambda_n \simeq \hbar\lambda_n^+$, the value of Γ_n could be calculated from Eq. (A3) if the matrix element $|M|^2$ were known, providing a connection between the lifetime of intermediate states and the strength of the two-body interaction. At present, no reliable estimates for $|M|^2$ are available, making it impossible to obtain a theoretical value for Γ_n.

An experimental value for the width can be obtained from the measurement of the cross section for pre-equilibrium emission. The cross section for emission from the first-formed intermediate state will be[25]

$$\sigma_{pe} = \sigma_{abs}\Gamma_{con}/\Gamma_n , \tag{A4}$$

where σ_{abs} is the absorption cross section, Γ_{con} is the continuum width of the intermediate state, and Γ_n is the total width of the intermediate (n-exciton) state. According to Williams[11] the width to the continuum of such a state is

$$\Gamma_{con}(\epsilon) = \frac{\mu_b \epsilon \sigma_{cap} \rho_{n-1}(U)}{\pi^2\hbar^2\rho_n(E^*)}, \tag{A5}$$

where σ_{cap} is the inverse capture cross section, and $\Gamma_{con}(\epsilon)$ is the width for emission of a particle of energy ϵ. Substituting this expression in Eq. (A4), the following expression is obtained:

$$\Gamma_n = \frac{\sigma_{abs}\mu_b\sigma_{cap}\rho_{n-1}(U)}{\pi^2\hbar^2\rho_n(E^*)[\sigma_{pe}(\epsilon)/\epsilon]} . \tag{A6}$$

If the lifetime of intermediate states is substantially longer than the single-particle transit time, an assumption which is consistent with the experimental estimates of Γ_n, then the analysis of Ericson and Strutinski[14] can be invoked to show that the angular distributions of particles emitted in pre-equilibrium reactions will be symmetric about 90°. The same equations which relate Γ/D to the transmission coefficient for compound states can be applied for an intermediate state; thus, one expects $\Gamma_{CN}/D_{CN} \sim \Gamma_{int}/D_{int}$, so if the compound states are strongly overlapping, the intermediate states will be also. Since the formula of Ericson and Strutinski applies if interference effects can be neglected and if the reaction proceeds through states of valid J, the intermediate-state contribution will be symmetric.

B. Definition of Effective Exciton Number

Because of the large changes in the level density as a function of exciton number n, both the predicted residual excitation energy and bombarding energy dependence of the pre-equilibrium cross section are sensitive to the value assumed for the exciton number of the first intermediate state formed. This presents a particular problem in the case of an α-induced reaction, since a case could be made for counting the initial state as a four-exciton state (from the standpoint of the target nucleus) or as an eight-exciton state (from the standpoint of the compound nucleus) in which case the initial state is a four-particle–four-hole state.

In order to define an effective exciton number, the role of this parameter in the pre-equilibrium calculation must be considered. As has been indicated, the density of final states of the system is a sensitive function of the exciton number, from which it follows that exciton counting cannot be based on nuclear-structure considerations, i.e., on a comparison of the given state to a specific ground state, but rather on a comparison between the given state and a "typical" n-exciton state.

The distribution of energy among the various excitons in an n-exciton state can be evaluated by examining the properties of the expression $\rho_1(U_1)\rho_{n-1} \times (E - U_1)$; it can easily be shown that the distribution of energies of the individual excitons has a narrow peak at E/n. Because the initial state in an α-induced reaction is one in which all of the energy is shared by four excitons, it resembles a four-exciton state more than an eight-exciton state in terms of the distribution of energy. Stated in another way: only excitons with energy correspond to degrees of freedom of the system while excitons at or near the ground state have relatively little influence on transition rates and lifetimes because of the small number of final states available to them. These same arguments indicate that the difference between exciton numbers for odd-even and even-even nuclei predicted by Griffin[9] may be significantly reduced.

Such an analysis does not in general give the value of n corresponding to the first term of the series in Eq. (6), but rather the value of n for the first intermediate state formed. For the (p,n) reaction it is expected that the first intermediate state could decay with the emission of a neutron, but for the (α,n) reaction it is not clear that in one two-body interaction the neutron could acquire enough energy so that the other three nucleons remain bound. If additional interactions are necessary, the n for the first term of Eq. (6) will be larger than that for the first-formed intermediate state.

*Work performed under the auspices of the U. S. Atomic Energy Commission.

[1]N. O. Lassen and V. A. Sidorov, Nucl. Phys. 19, 579 (1960).
[2]V. A. Sidorov, Nucl. Phys. 35, 253 (1962).
[3]R. Sherr and F. P. Brady, Phys. Rev. 124, 1928 (1961).
[4]C. Wong, J. D. Anderson, J. W. McClure, and B. D. Walker, Nucl. Phys. 57, 515 (1964).
[5]R. M. Wood, R. R. Borchers, and H. H. Barschall, Nucl. Phys. 71, 529 (1965).
[6]R. W. West, Phys. Rev. 141, 1033 (1966).
[7]D. Bodansky, Ann. Rev. Nucl. Sci. 12, 79 (1962).
[8]V. F. Weisskopf, Phys. Rev. 52, 295 (1937).
[9]J. J. Griffin, Phys. Rev. Letters 17, 478 (1966).
[10]M. Blann, Phys. Rev. Letters 21, 1357 (1968).
[11]F. C. Williams, Jr., Phys. Letters 31B, 184 (1970).
[12]M. Blann and F. M. Lanzafame, Nucl. Phys. A142, 559 (1970); W. W. Bowman and M. Blann, *ibid.* A131, 513 (1969).
[13]J. D. Anderson and C. Wong, Nucl. Instr. Methods 15, 178 (1962); B. D. Walker, J. D. Anderson, J. W. McClure, and C. Wong, *ibid.* 29, 333 (1964).
[14]T. Ericson and V. Strutinski, Nucl. Phys. 8, 284 (1958).
[15]J. J. Griffin, Phys. Letters 24B, 5 (1967).
[16]T. Ericson, Advan. Phys. 9, 425 (1960).
[17]P. E. Hodgson, in *Proceedings of the International Conference on Direct Interactions and Nuclear Reaction Mechanisms, Padua, Italy, 1962,* edited by E. Clementel and C. Villi (Gordon & Breach Publishers, Inc., New York, 1963), p. 103.
[18]J. Benveniste, G. Merkel, and A. Mitchell, Phys. Rev. 141, 980 (1966).
[19]M. A. Preston, *Physics of the Nucleus* (Addison-Wesley Publishing Company, Inc., Reading, Massachusetts, 1962), p. 513.
[20]L. F. Hansen and R. D. Albert, Phys. Rev. 128, 291 (1962).
[21]E. G. Bilpuch, K. K. Seth, C. D. Bowman, R. H. Tabony, R. C. Smith, and H. W. Newson, Ann. Phys. (N.Y.) 14, 387 (1961).
[22]M. J. Fluss, J. M. Miller, J. M. D'Auria, N. Dudley, B. M. Foreman, Jr., L. Kowalski, and R. C. Reedy, Phys. Rev. 187, 1449 (1969).
[23]J. R. Huizenga, H. K. Vonach, A. A. Katsanos, A. J. Gorski, and C. J. Stephan, Phys. Rev. 182, 1149 (1969).
[24]T. Ericson, Nucl. Phys. 11, 481 (1959).
[25]This expression follows directly from Eqs. (2.85) and (2.86) of H. Feshbach, A. K. Kerman, and R. H. Lemmer, Ann. Phys. (N.Y.) 41, 230 (1967).

PHYSICAL REVIEW C VOLUME 3, NUMBER 2 FEBRUARY 1971

Study of the Level Structure of ^{50}Ti and ^{51}Ti Using the ^{49}Ti(n, γ) and ^{50}Ti(n, γ) Reactions

J. Tenenbaum, R. Moreh, and Y. Wand
Nuclear Research Center, Negev, Beer Sheva, Israel

and

G. Ben-David
Soreq Research Center, Yavne, Israel and Bar-Ilan University, Ramat-Gan, Israel

(Received 10 August 1970)

The capture γ-ray spectrum resulting from thermal-neutron capture in ^{49}Ti and ^{50}Ti has been measured using a 30- and a 10-cm^3 Ge(Li) detector, and angular-correlation measurements were carried out using NaI(Tl) detectors. Some 16 γ lines corresponding to transitions between levels of ^{50}Ti, and 9 γ lines corresponding to transitions between levels of ^{51}Ti were observed. The neutron separation energies of ^{50}Ti and ^{51}Ti were determined to be 10.938 $\pm$0.008 and 6.377 $\pm$0.007 MeV, respectively. The following assignments of spins for some levels (in MeV) of ^{50}Ti and the first excited level of ^{51}Ti were made: 1.555 (2^+), 2.675 (4^+), 4.151 [$2^+, 3^+, 4^+, (5^+)$], 4.178 ($2^+, 3^+, 4^+$), 4.887 [$2^+, 3^+, 4^+, (5^+)$], 5.195 ($2^+, 3^+, 4^+$), 5.382 [$2^+, 3^+, 4^+, (5^+)$], 5.948 [$3^+, 4^+, (5^+)$] for ^{50}Ti and 1.164 ($\frac{1}{2}^-$) for ^{51}Ti. There are some indications that only the 3^- capture-state spin contributes to the population of the low-lying levels in ^{50}Ti. The results of a comparison between the measured strengths of exciting the ^{50}Ti levels in the (n, γ) and (d, p) reactions are discussed.

I. INTRODUCTION

In two previous papers,[1,2] we have reported the results from the (n, γ) reaction on ^{46}Ti and ^{47}Ti. In the present paper, the (n, γ) reaction on ^{49}Ti and ^{50}Ti was used for investigating the energy levels of ^{50}Ti and ^{51}Ti and for further study of the reaction mechanism of the (n, γ) process. The results are discussed in the light of recent studies made by other investigators. These studies employed the ^{49,50}Ti(d,p),[3] ^{50}Ti(p,p'),[4] ^{48}Ti(t,p),[5] and ^{49}Ti(t,p)[6] reactions. In particular, using the (d,p) reaction, it was possible to identify all the single-particle states associated with the $2p_{3/2}$, $2p_{1/2}$ shells as well as other shells such as $1f_{7/2}$, $2d_{3/2}$, $3s_{1/2}$, and $1f_{5/2}$ in both those nuclei.